ISSN 1547-4771, Physics of Particles and Nuclei Letters, 2020, Vol. 17, No. 2, pp. 204–210. © Pleiades Publishing, Ltd., 2020.

PHYSICS AND TECHNIQUE OF ACCELERATORS

Experimental Validation of the Field and Beam Dynamics Simulations for a Superconducting Cyclotron

V. Smirnov[a], *, S. Vorozhtsov[a], X. Wu[b], D. Alt[b], G. Blosser[b], G. Horner[b], J. Paquette[b], N. Usher[b], J. Vincent[b], and Z. Neville[c]

[a] *Joint Institute for Nuclear Research, Dubna, Russia*
[b] *Ionetix Corporation, Lansing, Michigan, USA*
[c] *Disher Corporation, Zeeland, Michigan, USA*
**e-mail: vsmirnov@jinr.ru*

Received November 15, 2019; revised November 15, 2019; accepted November 18, 2019

Abstract—The Ion-12SC is a sub-compact, 12.5 MeV proton super-conducting isochronous cyclotron for commercial medical isotope production recently developed at Ionetix Corporation. The machine features a patented cold steel and cryogen-free conduction cooling magnet, a low power internal cold-cathode PIG ion source, and an internal liquid target. It is designed to produce N-13 ammonia for dose on-demand cardiology applications but can also be used to produce F-18, Ga-68 and other medical isotopes widely used in Positron Emission Tomography (PET). The cyclotron is being installed and commissioned at several medical centers. During the initial machine operating periods, some issues appeared. In particular, imperfections in manufacturing and assembly of the magnet introduced unwanted low order magnetic harmonics that resulted in beam losses. This report presents results of analysis of the measured magnetic field and beam dynamics in the cyclotron that were initiated to solve the problem. The calculations led to a process for implementing compensating magnetic shims to improve the beam transmission.

Keywords: cyclotron, beam dynamics, calculations, measurements
DOI: 10.1134/S154747712002020X

1. INTRODUCTION

The Ion-12SC [1, 2] is a 12.5 MeV, 10 μA, proton superconducting cyclotron. This is the world's smallest commercial cyclotron applied to medical isotope production. To aid in field shaping and reduce the need for shimming, the warm iron 3-spirals sectored poles are manufactured of Armco pure iron. The final energy radius of 115 mm was arrived at as a qualitative compromise between machine size and required peak RF voltages. The system is designed to irradiate an internal liquid target for isotope production positioned at 140 mm radially. The target is positioned where maximum turn separation exists 180° opposite to the added 1st harmonic static valley shim. The machine features a patented cold steel yoke and pole design [3] in conjunction with warm iron spiraled focusing sectors. The design was applied such that the magnetic yoke is in thermal contact with the superconducting coils (Fig. 1).

The cold steel design simplifies the magnet construction eliminating additional room for superinsulation between the coil and the yoke. A warm bore through the magnet provides the mounting surfaces for the warm iron sectored poles and for accommodation of the ion source, RF resonator, internal target, and other equipment as is needed.

The installed weight of the system is less than 2.3 t, and requires less than 34 kW operating power resulting in a significant advantage over existing machines where space and power are important such as in single-site dose-on-demand operations. The superconducting magnet is conduction cooled, cryogen free design cooled by a single pulse tube cryo-cooler. It is normally left continuously charged in persistence mode for months at a time and requires approximately five hours to charge and 3 h to discharge. Several of these machines have already been built and deployed. The Ionetix manufacturing facility is capable of producing up to 30 machines per year.

The continuous R&D efforts in physics and engineering have been made to improve the machine performance, stability and reliability. The magnetic field is mapped with a Hall-probe based mapper to accurately measure the isochronism and provide information needed to compensate for any unwanted 1st harmonics.

2. BEAM INTENSITY TRACE

Analysis of the measured magnetic field map and following beam dynamics simulation show that in many cases the 1st harmonics of the magnetic field

Fig. 1. Cyclotron installation with the equipment around shown.

leads to the orbit moving off center preventing acceleration to full energy and intensity. The magnitude of these unwanted harmonics is small and may be compensated for by appropriate shimming in the center of the field. The amplitude of the measured magnetic field 1st harmonics is less than ~20–30 Gs for all constructed cyclotrons, which is relatively small given 4.5 T magnitude of the central magnetic field. It is believed that in given cyclotron the so-called gap crossing resonance [4, 5] takes place due to a different azimuthal periodicity of the magnetic and electric field distributions resulting in decentering of the orbits. The magnetic field of the cyclotron has 3-fold spiral structure, and the RF system with one dee and 2 accelerating gaps is of 2-fold structure. The distribution of the 1st harmonics amplitude along the radius is about the same for all Ion-12SC cyclotrons. To improve the machine performance, a number of actions were taken including analysis of the magnetic field measurements, beam acceleration simulations, discovery of the beam transmission problems, and formulation of the possible field corrections for a specific magnetic system. The magnetic field map was measured in the cyclotron midplane on a rectangular grid with 5 mm spacing. To increase the resolution in the analysis a cubic interpolation has been applied.

A number of possible effects on mapper accuracy were explored. The most significant effects came from ensuring the sample grid was accurately centered on the field. Otherwise, this would result in artificial harmonic content from the field map. The iteration process was applied to define the offsets of the mapper coordinates. These were subtracted from the measurement coordinates to properly align the data. Minimization of the 1st magnetic harmonics in the resulting map was a criterion for the process termination. The field map obtained in this manner was used to analyze the beam dynamics. It was shown that the average magnetic field deviated from the required one by less than $\pm 0.05\%$ (Fig. 2).

Figure 3 gives the measured dependence of the amplitude of the 1st magnetic harmonics vs. radius. The simulations show that in spite of reasonable beam transmission efficiency (~20%) in the central region, the total transmission from the ion source to the final radius is very low. During the acceleration process the losses of the particles on the vacuum chamber wall and on other structure elements takes place due to the orbit moving off center. The analysis shows that this effect cannot be completely compensated for a corresponding ion source shift from its central position.

If the first harmonic is analytically removed from the measured field maps, acceleration to full energy and intensity is obtained resulting in ~100% beam transmission in the expected region. To compensate for the existing 1st magnetic harmonics, a set of the steel shims was designed to be installed in the axial gap between the sectors as shown in Fig. 4. The introduced set of the shims allows reduction of the 1st magnetic harmonics amplitude in the whole working radial range. In calculations this yields the required increase of the beam transmission from the ion source to the production target. It was found that the main positive effect on the beam transmission comes from the com-

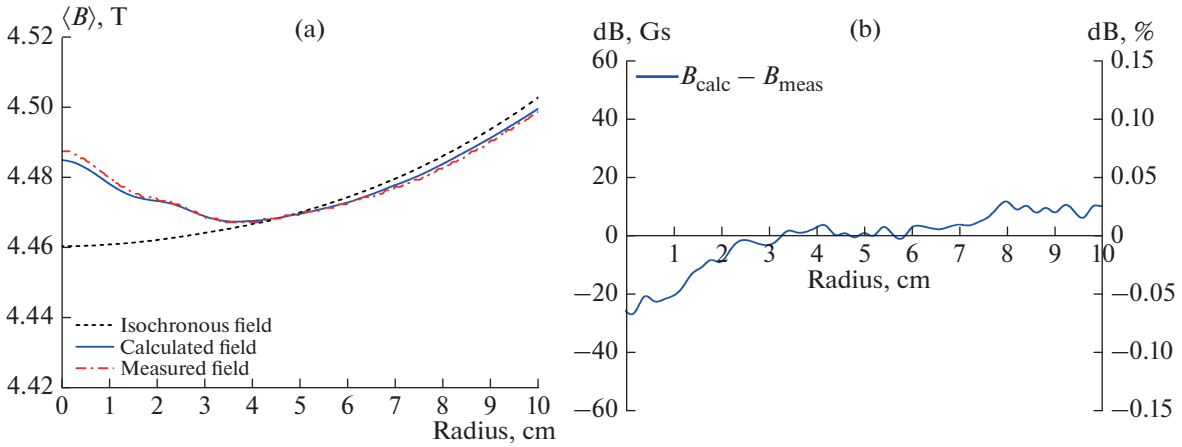

Fig. 2. Average field vs. the isochronous field (left) and the difference between these curves (right).

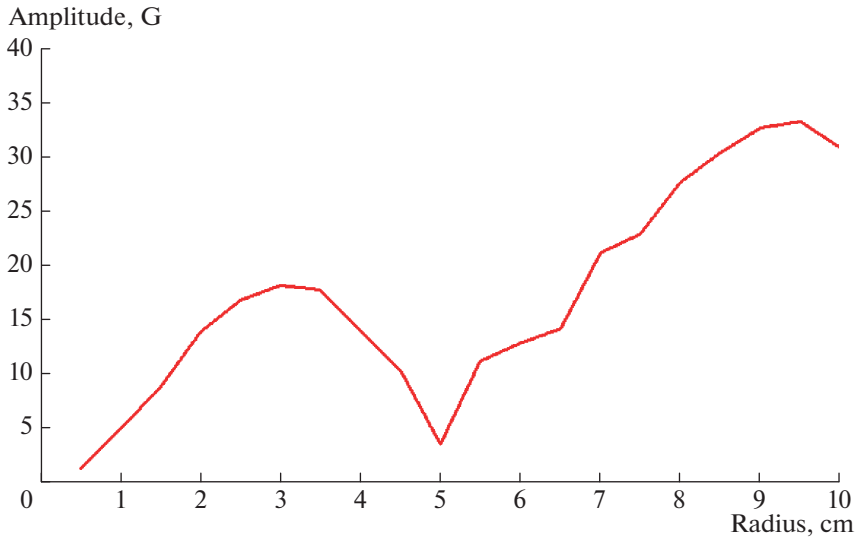

Fig. 3. Amplitude of 1st harmonic in the measured magnetic field.

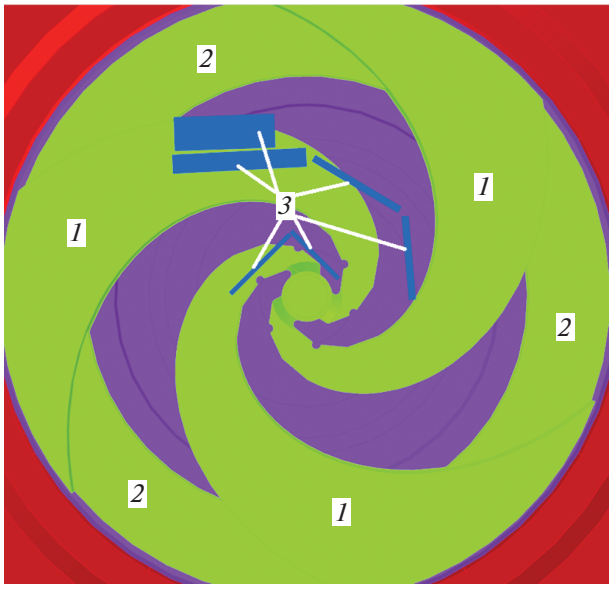

Fig. 4. Set of steel shims foreseen for correction of the 1st magnetic harmonics: (*1*) sector, (*2*) valley shim, (*3*) compensation shims.

pensation of the 1st magnetic harmonics on initial turns. So, it was sufficient to install only a pair of the steel shims sitting in the central region [2]. Additionally, the effect of the ion source radial shift also gets more pronounced in this case. However, the ion source positioning is allowed only along the acceleration gap of the dee (X-axis in Fig. 4). The total beam transmission reaches ~15% for the optimal ion source position off-center. This optimal transmission efficiency will be reduced by 40 or by 80% if the ion source is shifted from its optimal position along X-axis by 0.5 mm either in the positive or in negative direction. As a result of the optimization described above the measured beam transmission enhancement can be seen in Fig. 5. In the beam tests, the beam probe can cover the radial path from 46 mm to 151 mm, and can be fitted with a carbon block (intensity probe head) or stack of thin borosilicate glasses (energy probe head) for the beam current or energy measurement during the commissioning. The port on the opposite side of the RF system is used for the beam probe insertion.

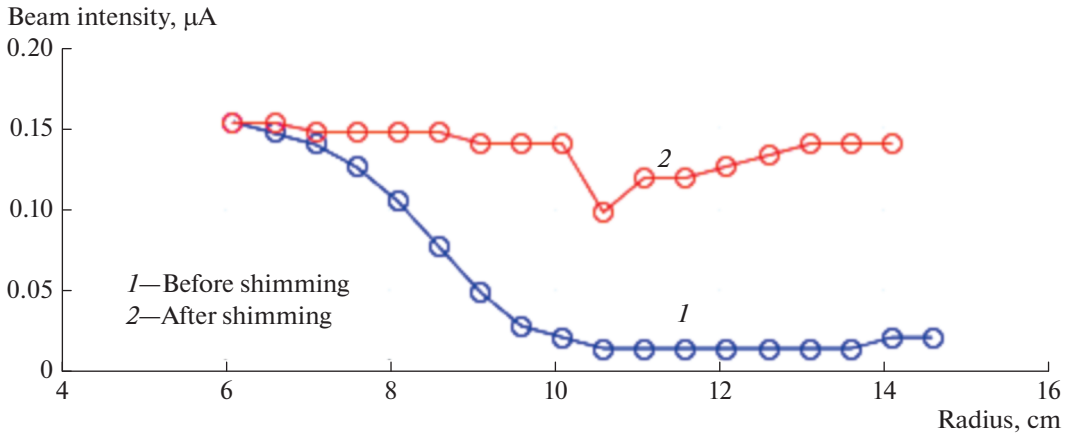

Fig. 5. Measured beam intensity before and after correction of the first harmonics.

3. ANALYSIS OF BEAM AXIAL DISPLACEMENT

The beam current probe has axial size of ±4 mm centering on the median plane of the cyclotron. The probe is surrounded by the jaws to register the accelerated particles with axial displacement off the median plane in 4–5 mm range (Fig. 6). The arrangement permits estimation of the axial displacement of the beam along the working radial range. Additionally, the viewer probe gives visual information on the beam spot.

Readings of the beam current and viewer probes are shown in Figs. 7 and 8. But the viewer gets easily saturated, and one has to run at a much lower intensity level. So, it is necessary to use the beam current probe data, which gives more accurate information. The viewer should be used just to have general ideas of the beam position.

An analysis of the beam measurements shows that an axial shift of the beam takes place during the acceleration process in a majority of the working radial range. The effect leads to a substantial intensity reduction of the beam impinging on the production target. The reason of particle losses could be an axial displacement of the magnetic median plane in the cyclotron. The most pronounced effect took place for the machine version locally named as T5. There, the beam axial displacement was observed in the whole radial range (Fig. 8).

For interpretation of the observed effects and finding the way for possible improvements a set of the beam dynamics simulations were performed. The corresponding displacements of the structure elements were taken into account in the calculations of the spatial magnetic field distribution used in the beam simulations. The ultimate goal of the simulations was to define such displacements that have an impact on the beam similar to that observed in the measurements.

To get an impression of the vertical position of the beam center of mass, a useful analytical expression from [6] can be applied:

$$z_{\text{beam}}(r) = -\frac{r}{B_{\text{tot}}}\frac{\partial B_z^{\text{coil}}}{\partial r}\frac{1}{Q_z^2}\delta, \qquad (1)$$

where, δ is axial shift of the coil, $\partial B_z^{\text{coil}}/\partial r$ is radial derivative of the coil contribution to the axial component of the field, Qz is axial betatron frequency, B_{tot} is total azimuthally mean magnetic field. Despite of low axial betatron frequency the resulting beam shift is not so pronounced due to small magnitude of the radial derivative of the field in the formula above (Fig. 9). In figure it can be seen that for the coil shift of 0.5 mm the beam axial offset is less than 1 mm.

Apparently, there are many combinations of the axial shifts and rotations of the coils that can produce intended perturbations of the beam axial dis-

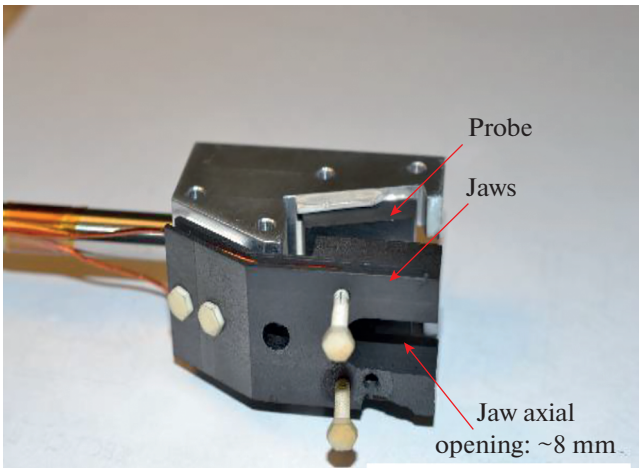

Fig. 6. Ion-12SC beam current probe.

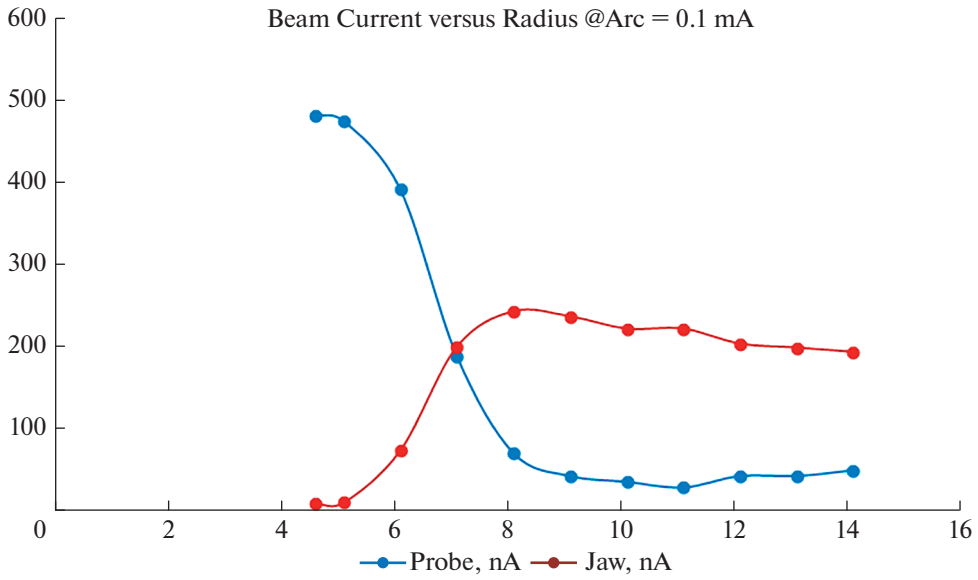

Fig. 7. Beam intensity probe trace.

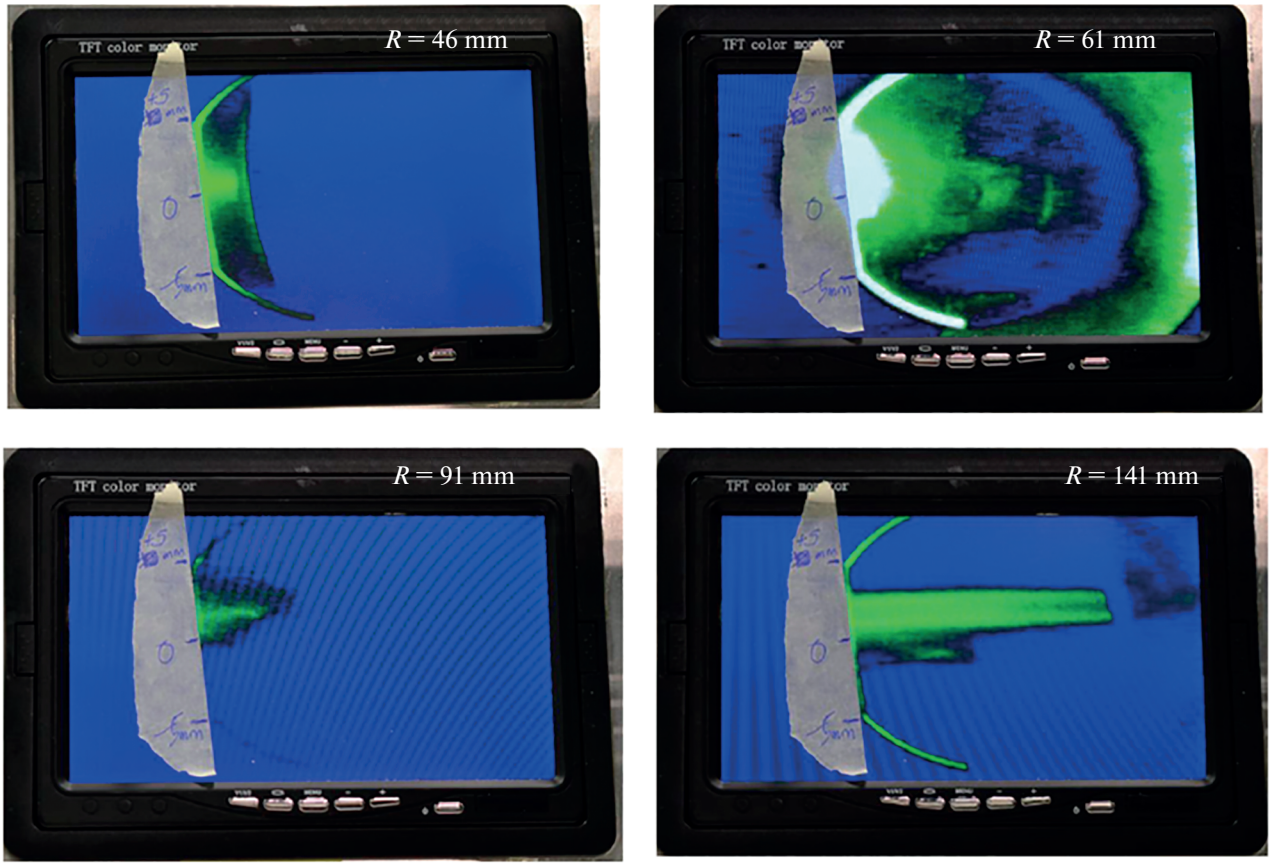

Fig. 8. Viewer probe image of the beam.

placement along the radius. The beam displacement obtained in this way can even change the sign in some cases depending on the sign of $\partial B_z^{\text{coil}}/\partial r$. Additionally, shifts and rotations of the iron mass near the median place can also induce some perturbations of the beam position. So, it's not a trivial

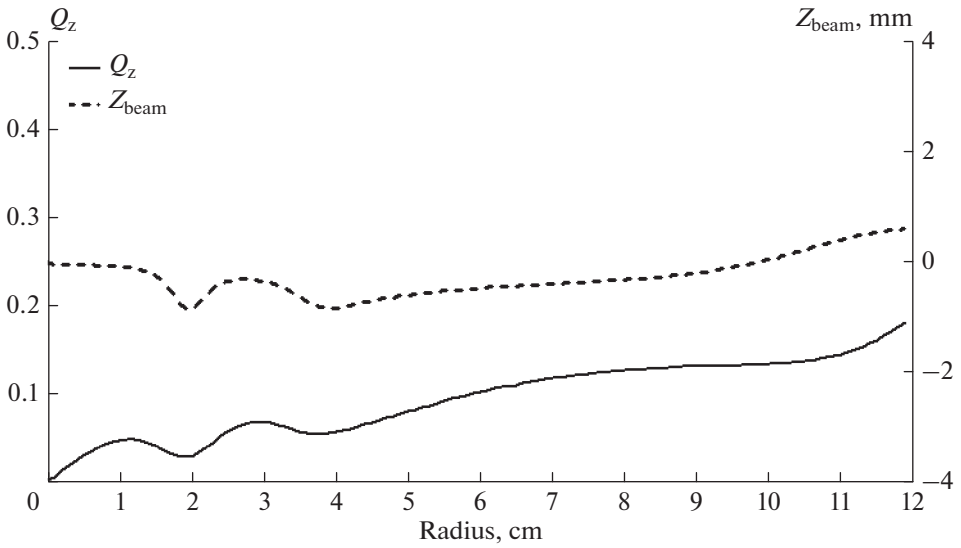

Fig. 9. Axial beam position as a function of radius from Eq. (1) with the coil shift by 0.5 mm (dash line). Solid line: axial betatron frequency dependence on radius.

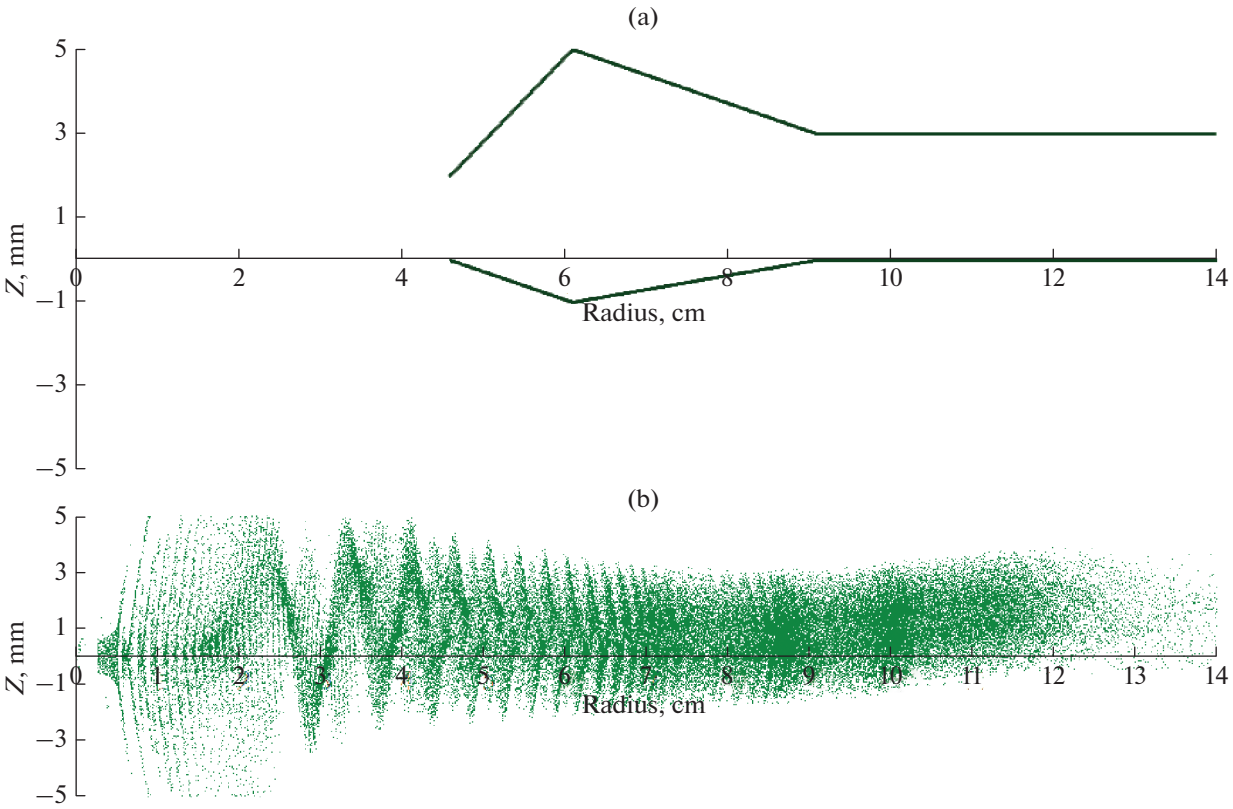

Fig. 10. Comparison of the beam envelope measurement (a) with the simulation (b) for the structure having axial shift of the coil and the valley shim.

task to find a unique combination of the coil and iron shifts and rotations to reassemble the beam shift behavior in the measurements. The situation is even more complex due to the inverse problem not being unique with multiple solutions. Nevertheless, we have found one solution which is in some sense close to that in the measurements. To this end, the coil was shifted axially by 1 mm and the valley shim by 2 mm. The beam behavior obtained in this way is shown in Fig. 10.

4. CONCLUSIONS

A set of operational Ion-12SC machines has been produced by the Ionetix manufacturing facility. The obtained beam intensity on the target is well within reach of the design goal. R&D efforts in physics and engineering to improve the machine performance, stability and reliability required extensive computer simulations including analysis of the measured magnetic fields and beam dynamics modeling. This activity allowed predicting some of the beam loss mechanisms and then determining methods to mitigate them by tailoring the magnetic field to increase the beam intensity on the production target.

REFERENCES

1. J. Vincent, G. Blosser, G. Horner, K. Stevens, N. Usher, X. Wu, S. Vorozhtsov, and V. Smirnov, "The ionetix ion-12SC compact superconducting cyclotron for production of medical isotopes," in *Proceedings of Cyclotrons'16, Zurich, Switzerland, 2016.*
2. X. Wu, D. Alt, G. Blosser, G. Horner, J. Paquette, N. Usher, and J. Vincent, "Recent progress in R&D for ionetix ion-12SC superconducting cyclotron for production of medical isotopes," in *Proceedings of IPAC2019, Melbourne, Australia*.
3. T. Antaya, "Compact, cold, superconducting isochronous cyclotron," US Patent No. US8558485 (2013).
4. M. M. Gordon, "The electric gap-crossing resonance in a three-sector cyclotron," Nucl. Instrum. Methods Phys. Res. **18** (19), 268–280 (1962).
5. H. Yao, R. Baartman, Y.-N. Rao, T. Zhang, and Yu. Lin, "Gap-crossing resonance in cyciae-100 cyclotron," in *Proceedings of CYCLOTRONS 2007 Conference, Giardini Naxos, Italy, 2007.*
6. J. M. Schippers, D. C. George, and V. Vrankovic, "Results of 3D beam dynamic studies in distorted fields of a 250 MeV superconducting cyclotron," in *Proceedings of CYCLOTRONS 2004 Conference, Tokyo, Japan, October 18–22, 2004,* p. 435.

SPELL: 1. ok